IEICE Electronics Express

A novel oversampling scheme for design of hybrid filter bank based ADCs

Xu Liu[1a)] **and Yingxiao Zhao**[2]

[1] *College of Electronic Science, National University of Defense Technology, No. 109, Deya Road, Changsha, Hunan 410073, China*

[2] *Science and Technology on Automatic Target Recognition Laboratory, National University of Defense Technology, No. 109, Deya Road, Changsha, Hunan 410073, China*

a) *liuxu199007@163.com*

Abstract: The parallel sampling structure of hybrid filter bank (HFB) has been considered as a promising candidate for realizing analog-to-digital conversion with high speed and high resolution simultaneously. However, the HFB design faces a challenge of accurately approximating the ideal synthesis filter frequency responses, which are discontinuous when the widely-adopted analysis filters are used. In this work, we analyze the origin of the ideal synthesis filter discontinuities. To address the discontinuity problem, we propose a novel oversampling scheme, i.e., artificially modifying the analysis filter frequency responses in the oversampling band. Performance evaluation reveals that the proposed oversampling scheme can significantly improve the HFB's reconstruction accuracy, while avoiding the existing methods' demerits such as the ill-conditioned coefficient matrix and the large reconstruction error in the oversampling band.

Keywords: analog-to-digital converter, hybrid filter bank, perfect reconstruction, discontinuity problem

Classification: Circuits and modules for electronic instrumentation

References

[1] M. Mishali, *et al.*: "Xampling: Analog to digital at sub-Nyquist rates" (Dec. 2009) [Online] Available: https://arxiv.org/abs/0912.2495.

[2] S. R. Velazquez, *et al.*: "Design of hybrid filter banks for analog/digital conversion," IEEE Trans. Signal Process. **46** (1998) 956 (DOI: 10.1109/78.668549).

[3] C. Lelandais-Perrault, *et al.*: "Wideband, bandpass, and versatile hybrid filter bank A/D conversion for software radio," IEEE Trans. Circuits Syst. I, Reg. Papers **56** (2009) 1772 (DOI: 10.1109/TCSI.2008.2008289).

[4] D. Asemani, *et al.*: "Subband architecture for hybrid filter bank A/D converters," IEEE J. Sel. Topics Signal Process. **2** (2008) 191 (DOI: 10.1109/JSTSP.2008.922469).

[5] S. H. Zhao and S. C. Chan: "Design and multiplierless realization of digital synthesis filters for hybrid-filter-bank A/D converters," IEEE Trans. Circuits Syst. I, Reg. Papers **56** (2009) 2221 (DOI: 10.1109/TCSI.2008.2012213).

DOI: 10.1587/elex.15.20180007
Received January 5, 2018
Accepted March 14, 2018
Publicized April 3, 2018
Copyedited April 25, 2018

[6] R. Gómez-García, *et al.*: "Mixed-domain receiver architecture for white space software-defined radio scenarios," 2012 IEEE International Symposium on Circuits and Systems (ISCAS) (2012) 822 (DOI: 10.1109/ISCAS.2012.6272167).
[7] J. P. Magalhães, *et al.*: "Bio-inspired hybrid filter bank for software-defined radio receivers," IEEE Trans. Microw. Theory Techn. **61** (2013) 1455 (DOI: 10.1109/TMTT.2013.2246184).
[8] B. Szlachetko: "Toward wide-band high-resolution analog-to-digital converters using hybrid filter bank architecture," Circuits Syst. Signal Process. **35** (2016) 1257 (DOI: 10.1007/s00034-015-0117-2).
[9] T. Liu, *et al.*: "Analysis and design of M-channel frequency-interleaved ADC with analog filter estimation," Analog Integr. Circuits Signal Process. **81** (2014) 173 (DOI: 10.1007/s10470-014-0381-2).
[10] L. Qiu, *et al.*: "Design of frequency-interleaved ADC with mismatch compensation," Electron. Lett. **50** (2014) 659 (DOI: 10.1049/el.2014.0577).
[11] L. Guo, *et al.*: "Analysis of channel mismatch errors in frequency-interleaved ADC system," Circuits Syst. Signal Process. **33** (2014) 3697 (DOI: 10.1007/s00034-014-9828-z).
[12] S. Soldado, *et al.*: "Controlling the reconstruction error in hybrid filter banks," 2011 IEEE 12th International Workshop on Signal Processing Advances in Wireless Communications (SPAWC) (2011) 46 (DOI: 10.1109/SPAWC.2011.5990454).

1 Introduction

Newly emerging communication technologies, such as the cognitive and software radios, exhibit a desire for high-speed, high-resolution analog-to-digital converters (ADCs) to implement wideband sampling. However, with current ADC fabrication techniques, it is difficult to manufacture an individual ADC that possesses high speed and high resolution simultaneously [1]. To overcome this bottleneck, a parallel sampling structure called hybrid filter bank (HFB) has been proposed [2], which has the potential to obtain a high overall sample rate from several low-speed ADCs while maintaining their high resolutions.

The proper operation of an HFB relies on the good matching between an analog analysis filter bank (AFB) and a digital synthesis filter bank (SFB), which are respectively responsible for segmenting and reconstructing the input wideband spectrum. For the design of HFB, almost all of the papers available recommend to firstly construct an AFB with easily-realizable (e.g., first- or second-order Butterworth) analog filters, then design a SFB to match the already constructed AFB [3, 4, 5, 6, 7, 8]. The SFB design process can be roughly divided into two steps: (1) Calculate the ideal synthesis filter frequency responses according to the perfect reconstruction (PR) equation; (2) Approximate the ideal synthesis filter frequency responses by finite impulse response (FIR) filters.

A problem occurs in the above HFB design process is that the ideal synthesis filter frequency responses are discontinuous at some frequencies [3]. These discontinuities make the ideal synthesis filters difficult to approximate by short FIR filters. In order to address the discontinuity problem, [3] proposes an oversampling scheme in which the oversampling band is assigned with a relatively small weight.

DOI: 10.1587/elex.15.20180007
Received January 5, 2018
Accepted March 14, 2018
Publicized April 3, 2018
Copyedited April 25, 2018

IEICE Electronics Express, Vol.15, No.8, 1–8

However, as pointed out in [4], this scheme results in an ill-conditioned coefficient matrix for the PR equation. Furthermore, large reconstruction errors will appear in the oversampling band, which has to be removed via a post-filtering procedure. A second-order cone programming method based on a similar oversampling scheme is used in [5, 9, 10, 11], but it also leads to large reconstruction errors in the oversampling band.

In this work, we analyze the origin of the ideal synthesis filter discontinuities. Basing on this, we propose a novel, simple but effective oversampling scheme, i.e., modifying the analysis filter frequency responses in the oversampling band. Performance evaluation reveals that this scheme can overcome the discontinuity problem while not increasing reconstruction errors in the oversampling band. Calculation of coefficient matrices' condition numbers demonstrates that all the coefficient matrices associated with our HFB design process are kept well-conditioned.

2 HFB model and discontinuity problem

The structure of an M-channel maximally decimated HFB is illustrated in Fig. 1. The input analog signal $x(t)$ (with a spectrum located within $[-\pi/T, \pi/T]$) is first segmented into M subbands by a bank of analog analysis filters $H_m(s)$ ($m = 1, \ldots, M$), then sampled by an ADC array at the rate of $1/MT$, where T is the sample period of the system. The digitized subband signals are then upsampled by a factor M, filtered by a bank of digital synthesis filters $F_m(z)$ ($m = 1, \ldots, M$), and finally summed together to reconstruct the input spectrum. The spectral representations of the input $x(t)$ and the output $\hat{x}[n]$ are denoted as $X(j\Omega)$ and $\widehat{X}(e^{j\omega})$, respectively.

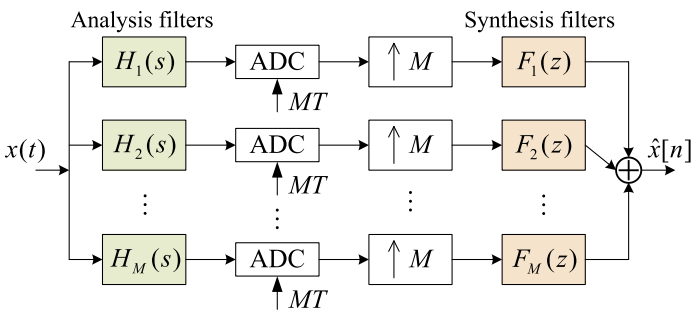

Fig. 1. Structure of an M-channel maximally decimated HFB.

To focus on the reconstruction errors caused by the mismatch between the AFB and the SFB, it is often assumed that the quantization noises originated from the parallel ADCs can be ignored [3, 4]. In this case, the HFB's output $\widehat{X}(e^{j\omega})$ can be written as

$$\widehat{X}(e^{j\omega}) = \underbrace{\frac{1}{T}\widetilde{X}(j\Omega)T_0(e^{j\omega})}_{\text{distortion term}} + \sum_{p=1}^{M-1} \underbrace{\frac{1}{T}\widetilde{X}\left(j\Omega - j\frac{2\pi p}{MT}\right)T_p(e^{j\omega})}_{\text{aliasing term}}\Bigg|_{\Omega=\omega/T}, \tag{1}$$

where $T_0(e^{j\omega})$ (called the distortion function) and $T_p(e^{j\omega})$ ($p = 1, \ldots, M-1$) (called the aliasing functions) are respectively defined as

DOI: 10.1587/elex.15.20180007
Received January 5, 2018
Accepted March 14, 2018
Publicized April 3, 2018
Copyedited April 25, 2018

IEICE Electronics Express, Vol.15, No.8, 1–8

$$\begin{cases} T_0(e^{j\omega}) = \dfrac{1}{M}\sum_{m=1}^{M} \widetilde{H}_m(j\Omega)F_m(e^{j\omega}), \\ T_p(e^{j\omega}) = \dfrac{1}{M}\sum_{m=1}^{M} \widetilde{H}_m\left(j\Omega - j\dfrac{2\pi p}{MT}\right)F_m(e^{j\omega}). \end{cases} \tag{2}$$

$\widetilde{X}(j\Omega)$ and $\widetilde{H}_m(j\Omega)$ are respectively the periodic extensions (with the period $2\pi/T$) of $X(j\Omega)$ and $H_m(j\Omega)$ limited to $[-\pi/T, \pi/T]$ [4]. The desired output of the HFB is the distortionless sampled version of the input signal, i.e., $X(j\Omega)|_{\Omega=\omega/T}$. Since the input $x(t)$ is assumed to be bandlimited in $[-\pi/T, \pi/T]$, here $\widetilde{X}(j\Omega)$ is simply $X(j\Omega)$. Therefore, according to Eq. (1), the PR condition for an HFB can be expressed as the following equation (called the PR equation)

$$\begin{cases} T_0(e^{j\omega}) = ce^{-j\omega d}, \\ T_p(e^{j\omega}) = 0 \quad (p = 1, \ldots, M-1), \end{cases} \quad \forall \omega \in [-\pi, \pi] \tag{3}$$

where c is a scale factor and d is the system delay. In practice, PR is generally not realizable. What a designer pursues is to approximate PR within a given tolerance, by properly designing the AFB and SFB.

To build an HFB, analog filters with the following low-order transfer functions are widely adopted as the AFB

$$\begin{cases} H_1(s) = \dfrac{\Omega_1}{s + \Omega_1}, \\ H_m(s) = \dfrac{Bs}{s^2 + Bs + \Omega_m^2} \quad (m = 2, \ldots, M), \end{cases} \tag{4}$$

where Ω_m $(m = 1, \ldots, M)$ denote the cutoff or resonation frequencies, B is the 3-dB passband width. For example, for a four-channel (i.e., $M = 4$) HFB, the frequency responses of its analysis filters are plotted in Fig. 2 (the solid lines).

Given the analysis filters of Eq. (4), the ideal synthesis filter frequency responses, i.e., the ones that perfectly match the analysis filters and can be obtained by solving the PR Eq. (3),[1] are always discontinuous at integral multiples of $2\pi/M$ [3]. For example, the ideal synthesis filter frequency responses that match the analysis filters in Fig. 2 (the solid lines) are plotted in Fig. 3(a), showing discontinuities at $\pm\pi/2$.

3 Origin of ideal synthesis filter discontinuities

We point out that the discontinuities of the ideal synthesis filter frequency responses originate from the analysis filters' non-zero phases at the border frequencies $\pm\pi/T$. This can be illustrated by the example as follows.

Suppose $\Delta\omega$ is a very small positive frequency interval. To simplify the notations, we use ω^- and ω^+ to represent $\omega - \Delta\omega$ and $\omega + \Delta\omega$ respectively, i.e., the left and right two frequencies close to ω, where ω is an arbitrary frequency. For a four-channel HFB, the PR equations at the frequencies $(\pi/2)^-$ and $(\pi/2)^+$ can be rewritten in the following matrix forms

[1]To speak more specifically, the PR Eq. (3) is often solved numerically at K (a sufficiently large number, e.g., $K = 512$) discrete frequency points equally spaced in $[-\pi, \pi]$ [3, 4]. Thus, what we really obtain are the K-point samples of the ideal synthesis filter frequency responses. The parameters in Eq. (3) are set as $c = 1$ and $d = 0$.

DOI: 10.1587/elex.15.20180007
Received January 5, 2018
Accepted March 14, 2018
Publicized April 3, 2018
Copyedited April 25, 2018

IEICE Electronics Express, Vol.15, No.8, 1–8

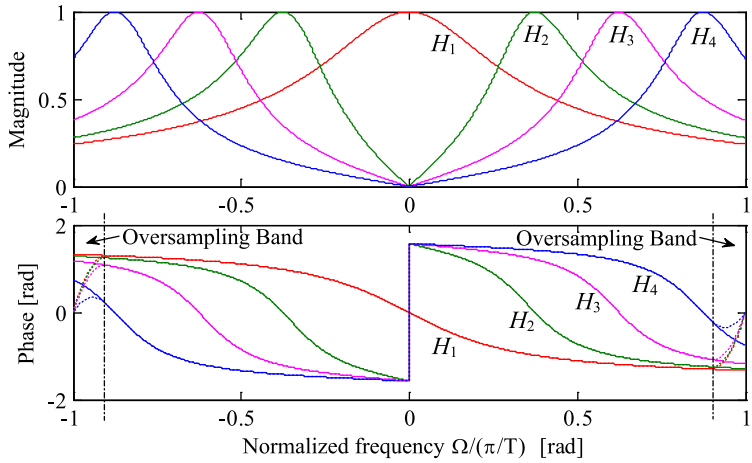

Fig. 2. Frequency responses of the analysis filters in a four-channel HFB. The solid lines are the original frequency responses. The dashed lines in the oversampling band (in the below panel) are the modified phase-frequency responses.

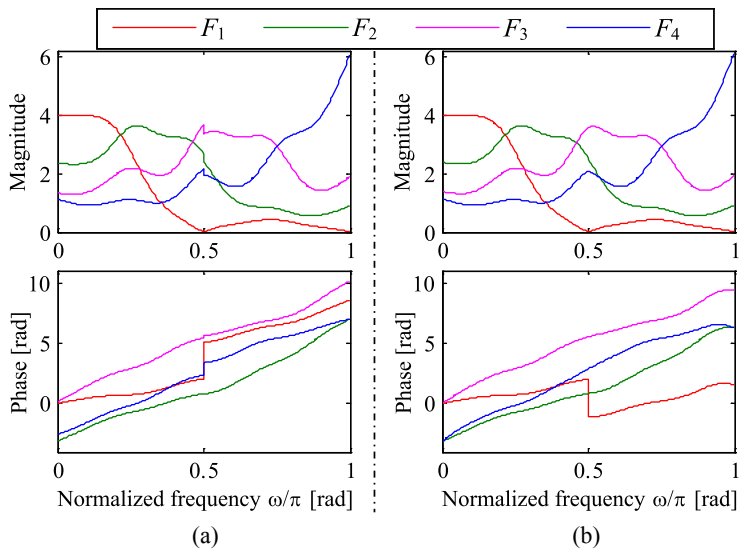

Fig. 3. Ideal synthesis filter frequency responses that match (a) the original analysis filter frequency responses and (b) the modified analysis filter frequency responses.

$$\mathbf{H}_1\mathbf{F}_1 = 4\mathbf{t}_1, \tag{5}$$

$$\mathbf{H}_2\mathbf{F}_2 = 4\mathbf{t}_2, \tag{6}$$

where $\mathbf{F}_1 = [F_1(e^{j(\frac{\pi}{2})^-}), F_2(e^{j(\frac{\pi}{2})^-}), \ldots, F_4(e^{j(\frac{\pi}{2})^-})]^T$, $\mathbf{F}_2 = [F_1(e^{j(\frac{\pi}{2})^+}), F_2(e^{j(\frac{\pi}{2})^+}), \ldots, F_4(e^{j(\frac{\pi}{2})^+})]^T$, $\mathbf{t}_1 = [ce^{-j(\frac{\pi}{2})^- d}, 0, 0, 0]^T$, $\mathbf{t}_2 = [ce^{-j(\frac{\pi}{2})^+ d}, 0, 0, 0]^T$, and

DOI: 10.1587/elex.15.20180007
Received January 5, 2018
Accepted March 14, 2018
Publicized April 3, 2018
Copyedited April 25, 2018

IEICE Electronics Express, Vol.15, No.8, 1–8

$$\mathbf{H}_1 = \begin{bmatrix} H_1\left(j\frac{\left(\frac{\pi}{2}\right)^-}{T}\right) & H_2\left(j\frac{\left(\frac{\pi}{2}\right)^-}{T}\right) & \dots & H_4\left(j\frac{\left(\frac{\pi}{2}\right)^-}{T}\right) \\ H_1\left(j\frac{0^-}{T}\right) & H_2\left(j\frac{0^-}{T}\right) & \dots & H_4\left(j\frac{0^-}{T}\right) \\ H_1\left(j\frac{\left(-\frac{\pi}{2}\right)^-}{T}\right) & H_2\left(j\frac{\left(-\frac{\pi}{2}\right)^-}{T}\right) & \dots & H_4\left(j\frac{\left(-\frac{\pi}{2}\right)^-}{T}\right) \\ H_1\left(j\frac{\pi^-}{T}\right) & H_2\left(j\frac{\pi^-}{T}\right) & \dots & H_4\left(j\frac{\pi^-}{T}\right) \end{bmatrix},$$

$$\mathbf{H}_2 = \begin{bmatrix} H_1\left(j\frac{\left(\frac{\pi}{2}\right)^+}{T}\right) & H_2\left(j\frac{\left(\frac{\pi}{2}\right)^+}{T}\right) & \dots & H_4\left(j\frac{\left(\frac{\pi}{2}\right)^+}{T}\right) \\ H_1\left(j\frac{0^+}{T}\right) & H_2\left(j\frac{0^+}{T}\right) & \dots & H_4\left(j\frac{0^+}{T}\right) \\ H_1\left(j\frac{\left(-\frac{\pi}{2}\right)^+}{T}\right) & H_2\left(j\frac{\left(-\frac{\pi}{2}\right)^+}{T}\right) & \dots & H_4\left(j\frac{\left(-\frac{\pi}{2}\right)^+}{T}\right) \\ H_1\left(j\frac{(-\pi)^+}{T}\right) & H_2\left(j\frac{(-\pi)^+}{T}\right) & \dots & H_4\left(j\frac{(-\pi)^+}{T}\right) \end{bmatrix}.$$

It can be seen that when $\Delta\omega \to 0$, the first three rows of $\mathbf{H}_1$ are equal to those of $\mathbf{H}_2$. The last row of $\mathbf{H}_1$ is always unequal to that of $\mathbf{H}_2$, unless the phases of $H_m(j\Omega)$ $(m = 1, \dots, 4)$ at $\pm\pi/T$ are zeros. On the other hand, $\mathbf{t}_1$ tends to be equal to $\mathbf{t}_2$ as $\Delta\omega \to 0$. Therefore, the solutions to Eq. (5) and Eq. (6), i.e., $\mathbf{F}_1$ and $\mathbf{F}_2$, are always discontinuous, unless the analysis filters have zero phases at $\pm\pi/T$.

4 Description of the proposed oversampling scheme

It is manifested in Section 3 that if the analysis filters satisfy the constraint that their phases tend to zeros when $\Omega \to \pm\pi/T$, then the ideal synthesis filter frequency responses will be continuous throughout the entire frequency band, i.e., $[0, \pi]$ (also $[-\pi, 0]$). This inspires us with the oversampling scheme described below, which can overcome the discontinuity problem.

We assume that the HFB operates in a slightly oversampling mode, specifically, the input signal $x(t)$ is supposed to be bandlimited to $[-(1-\alpha)\pi/T, (1-\alpha)\pi/T]$, where α $(0 < \alpha < 1)$ is seen as the oversampling ratio. Since there is no input signal in the oversampling band, i.e., $[-\pi/T, -(1-\alpha)\pi/T] \cup [(1-\alpha)\pi/T, \pi/T]$, the analysis filter frequency responses in this band have no effect on the HFB's output, thus they can be artificially modified to any form. Considering the origin of the discontinuity problem, we choose to modify the analysis filters' phases in the oversampling band such that they tend to zeros when $\Omega \to \pm\pi/T$.

To make smooth transitions at the connecting frequencies $\pm(1-\alpha)\pi/T$, we utilize quadratic curves as the modified phase-frequency responses in the oversampling band. For example, for the modified phase-frequency response for $H_1(j\Omega)$ in $[(1-\alpha)\pi/T, \pi/T]$, the quadratic function $Q_1(\Omega) = a_1\Omega^2 + b_1\Omega + c_1$ is used. The coefficients a_1, b_1, c_1 are determined by solving the following equations

DOI: 10.1587/elex.15.20180007
Received January 5, 2018
Accepted March 14, 2018
Publicized April 3, 2018
Copyedited April 25, 2018

IEICE Electronics Express, Vol.15, No.8, 1–8

$$\begin{cases} \left(\frac{\pi}{T}\right)^2 a_1 + \frac{\pi}{T} b_1 + c_1 = 0, \\ \left((1-\alpha)\frac{\pi}{T}\right)^2 a_1 + (1-\alpha)\frac{\pi}{T} b_1 + c_1 = \angle H_1\left(j(1-\alpha)\frac{\pi}{T}\right), \\ 2(1-\alpha)\frac{\pi}{T} a_1 + b_1 = \angle H_1'(j\Omega)|_{\Omega=(1-\alpha)\frac{\pi}{T}}, \end{cases} \tag{7}$$

where $\angle H_1'(j\Omega)$ is the first derivative of $\angle H_1(j\Omega)$ with respect to the pulsation Ω. In Eq. (7), the first and second equations refer to the phases at π/T and $(1-\alpha)\pi/T$, respectively, and the third equation refers to the curve's slope at $(1-\alpha)\pi/T$.

Conducting the above operation, the modified phases for the aforementioned analysis filters (shown in Fig. 2 with solid lines) are obtained and depicted in Fig. 2 with dashed lines (see the oversampling band in the below panel), when the oversampling ratio α is set to 10%. With the modified analysis filter frequency responses, the ideal synthesis filter frequency responses are recalculated and plotted in Fig. 3(b), which are continuous and smooth as expected.[2]

5 Performance evaluation

The ideal synthesis filter frequency responses shown in Fig. 3(b) are then approximated by four FIR filters of length $L = 128$,[3] thus the HFB design task is accomplished. Fig. 4 shows the reconstruction performance of this HFB. The distortion function has an almost unit magnitude (with a ripple of less than 0.01 dB) and a linear phase. The aliasing functions are below −79 dB throughout the entire band of $[-\pi, \pi]$, implying that the HFB has a spurious-free dynamic range (SFDR) of 79 dB. This HFB achieves a reconstruction performance com-

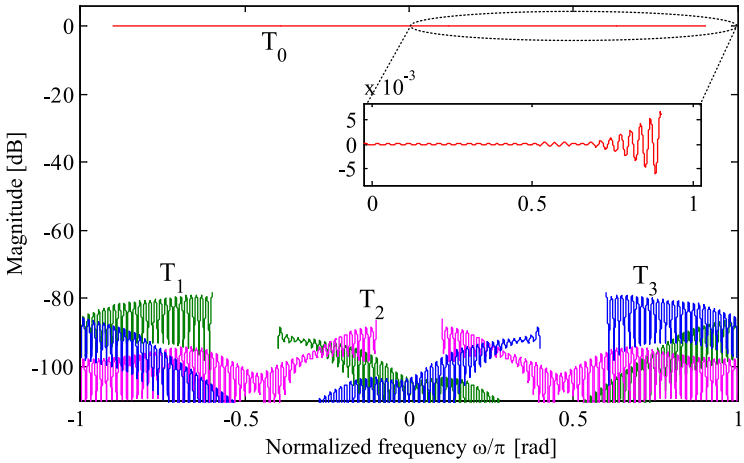

Fig. 4. Reconstruction performance of the four-channel HFB designed with the proposed oversampling scheme. An FIR filter of length $L = 128$ is utilized for each synthesis filter.

[2]Although a π-phase jump occurs for the ideal $F_1(e^{j\omega})$ at frequencies $\pm\pi/2$, it does not add the difficulty of approximating the ideal $F_1(e^{j\omega})$, because the magnitude of ideal $F_1(e^{j\omega})$ is zero at these frequencies.

[3]For each FIR filter, its L coefficients are obtained by truncating the K-point inverse fast Fourier transform (IFFT) of the ideal synthesis filter frequency response to the largest L consecutive values [2]. Note that since we set d to 0, the obtained FIR filters are noncausal. They should be further delayed by a time interval of $L/2$ to obtain the causal ones.

DOI: 10.1587/elex.15.20180007
Received January 5, 2018
Accepted March 14, 2018
Publicized April 3, 2018
Copyedited April 25, 2018

Table I. Achievable SFDRs of the HFBs with different FIR lengths

FIR length L	32	64	128	256	512
SFDR (dB), with modification	41	62	79	98	113
SFDR (dB), without modification	25	32	38	44	50

parable to those in [3, 5], without the need of post-filtering procedure for filtering out the oversampling band, which is however a necessity in [3, 5].

Table I presents the achievable SFDRs of the HFBs with different FIR lengths, in both cases of with and without modification to the analysis filters.[4] This table reveals the significant performance gain of the proposed oversampling scheme.

In the SFB design process, the PR Eq. (3) is often solved in its matrix-vectorial format (like Eq. (5) or Eq. (6)) at each discrete frequency point. To guarantee the robustness of the matrix equations' solutions, the coefficient matrices should be well-conditioned [12]. We check the condition numbers of the coefficient matrices associated with the modified analysis filters. All the condition numbers are less than 2.5, demonstrating that the coefficient matrices are well-conditioned.

6 Conclusion

In this work, we have proposed a novel oversampling scheme for HFB design. This scheme involves artificially modifying the analysis filter frequency responses in the oversampling band, the operation of which can eliminate the discontinuities of ideal synthesis filter frequency responses. Performance evaluation has shown that the proposed scheme can achieve a good reconstruction performance for HFB, without bringing about the demerits with existing oversampling schemes.

Acknowledgments

This work was supported in part by the National Natural Science Foundation of China under Grants 61502518, 61372099 and 61601480.

[4]For a fair comparison, an oversampling ratio of 10% is also assumed in the case of not modifying the analysis filters.

DOI: 10.1587/elex.15.20180007
Received January 5, 2018
Accepted March 14, 2018
Publicized April 3, 2018
Copyedited April 25, 2018